Optik 124 (2013) 607–612

Contents lists available at SciVerse ScienceDirect

Optik

journal homepage: www.elsevier.de/ijleo

Extracting parameters from slanted non-uniform gratings recorded in photopolymer. Part II: Experimental results

Dušan Sabol[a,b], Michael R. Gleeson[a], John T. Sheridan[a,*]

[a] UCD School of Electrical, Electronic and Communications Engineering, UCD Communication and Optoelectronic Research Centre, SFI Strategic Research Cluster in Solar Energy Conversion, College of Engineering and Architecture, Mathematical and Physical Sciences, University College Dublin, Belfield, Dublin 4, Ireland
[b] Slovak Institute of Metrology, Department of Thermometry, Photometry and Radiometry, Karlova Ves 63, 842 55 Bratislava, Slovakia

ARTICLE INFO

Article history:
Received 26 August 2011
Accepted 21 December 2011

Keywords:
Non-uniform grating
Slanted gratings
Photopolymer
Coupled-wave theory
Volume holography

ABSTRACT

In Part I of this paper the modelling of diffraction by non-uniform volume grating was examined. In Part II slanted volume gratings are recorded in PVA/AA based photopolymer material layers and both the grating growth curves and off-Bragg angular scans are measured. Best fits to the resulting experimental data, using the non-uniform diffraction model previously described, are performed and the grating parameters which give the best fits to these data curves are identified. The quality of these fits is quantified using the root mean square error.

1. Introduction

In Part I of this paper we have derived and numerically examined the predictions of first-order coupled wave theory using the Beta Value Method (BVM) for non-uniform gratings. In Part II the exact numerical model is applied to analyse experimental data obtained from gratings recorded in green sensitised PVA/AA photopolymer for various recording geometries, i.e., for transmission gratings recorded having different slant angles. In this way the grating profile recorded can be identified and information about the green sensitive PVA/AA based photopolymer material can be found in [1].

This paper is organised as follows: in Section 2 the experimental procedure is defined and effects on the recorded grating due to the particular recording and probing geometry are discussed. Section 3 describes three approaches, which were used to obtain the layer thickness estimation, and the numerical fitting procedures applied to extract the key grating parameters. A brief conclusion is presented in Section 4.

2. Experimental results

Experiments to measure angular scan data involve: (i) grating recording, and (ii) measurement of the resulting angular replay scan. The experimental setup shown in Fig. 1 was employed to perform both tasks. The photopolymer layer was exposed to two equally intense plane recording beams, I_1 and I_2, at wavelength $\lambda = 532\,\text{nm}$ (green), having total intensity $I_1 + I_2 = 4\,\text{mW/cm}^2$. At first, unslanted transmission gratings were recorded as shown in Fig. 2(a), and their angular scans measured. Then slanted gratings were recorded in the layer using a simple procedure which involves rotating the photopolymer layer before exposure, i.e., by making a pre-exposure rotation of Ω degrees, as shown in Fig. 2(b). The resulting slanted grating is then replayed using a probing beam as shown in Fig. 2(c). The relationship between the pre-rotation and incident angles for the unslanted and slanted geometries are described using

$$\theta_i^j = \hat{\theta}_i^j + \Omega, \tag{1}$$

where, as throughout the Part I, subscript $i\,(0, -1)$ denotes the transmitted and diffracted beams respectively and the superscript $j\,(E, R)$ denotes either an exposing or a replay beam. The symbol '^' is used to denote angles associated with the unslanted geometry, while Ω is the pre-exposure rotation angle. We note that the angles values presented are those measured in air.

The use of the pre-exposure rotation technique has several effects on the written grating: (i) different Fresnel reflection coefficients for the reference and object beams leads to variation of the fringe visibility, V, for the differently slanted grating exposures, and (ii) both exposing beams will refract differently according to Snell's law leading to variations in the grating period, Λ, for different slant angles. This means that the resulting grating slant angle, φ, achieved

* Corresponding author. Tel.: +353 1 716 1927; fax: +353 1 283 0921.
E-mail address: john.sheridan@ucd.ie (J.T. Sheridan).

0030-4026/$ – see front matter © 2012 Elsevier GmbH. All rights reserved.
doi:10.1016/j.ijleo.2012.01.003

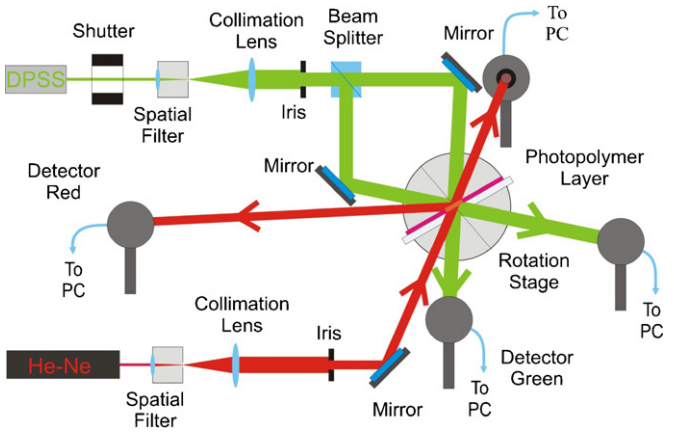

Fig. 1. Experimental setup – grating recording.

is smaller than the magnitude of the pre-exposure rotation, $\varphi < \Omega$, and also that the grating period increases with increasing amount of the pre-rotation, $\Lambda_1(\Omega_1) < \Lambda_2(\Omega_2)$, if $\Omega_1 > \Omega_2$.

The exposing time for all the cases presented in this study was 8 s. A spatial frequency of 1428 lines/mm in the unslanted geometry was used. This corresponds to equal exposing angles of incidence, of the reference and object exposing beams of $\theta_0^E = -\theta_{-1}^E = 22.32^\circ$ in air and of 14.07° inside the photopolymer layer. The average refractive index of the photopolymer was measured to be $n_{av} = 1.495$ [2], which is very close to the index of the glass substrate of $n \approx 1.5$. Therefore, in this study only beam propagation through two different media (air/photopolymer) is considered.

The process of grating evolution, during and after exposure, was continuously monitored using a red probe beam, at wavelength 633 nm, which is not absorbed by the photosensitiser, Erythrosine B, and thus does not affect the formation of the grating [3]. The transmitted intensities of both exposing beams as well as both the transmitted and diffracted probe beams were measured.

A typical example of the temporal evolution of the diffraction efficiency of the probing beam (growth curve) for the unslanted case is shown in Fig. 3. After the grating had been recorded and

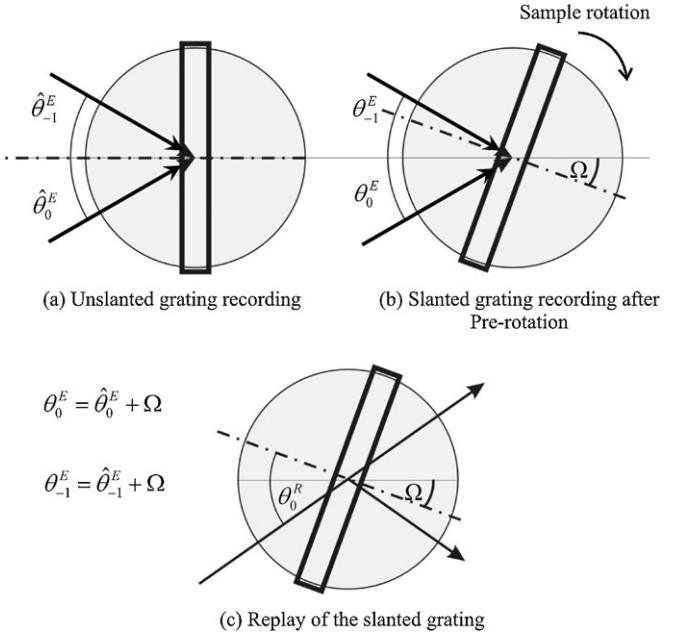

Fig. 2. Process of the photopolymer layer pre-rotation, (a) an unslanted grating, (b) recording of a slanted grating, (c) replay of the slanted grating.

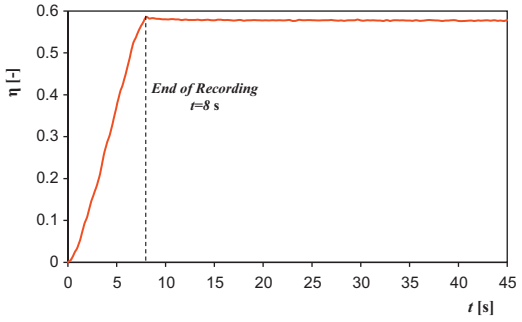

Fig. 3. Growth curve of an unslanted grating.

stabilized (once negligible post-exposure decay of the growth curve takes place), the grating was rotated over the replay angle range $\Delta\theta_0^R = \pm 3^\circ$ about the Bragg angle while constantly probing. Angular scans of the transmission and diffraction efficiencies in the red were thus obtained. Experimental angular scan data for the slanted gratings, which were recorded having pre-exposure rotation values of 0°, −10°, +10° and +20°, are shown in Figs. 4–7, together with the corresponding theoretical fits using Eqs. (40a) and (40b) presented in the Part I. All angular scans are plotted as a function of the difference angle, $\delta\theta_0^R$, between the probing incident angle and the on-Bragg replay angle for the unslanted geometry modified by the pre-exposure rotation angle, i.e.,

$$\delta\theta_0^R = \theta_0^R - (\widehat{\theta}_{0B}^R + \Omega). \tag{2}$$

The fitting procedure used and the resulting extracted parameters of the gratings are discussed in detail in Section 3, while assessment of the presented angular scans is going to continue in the next paragraphs.

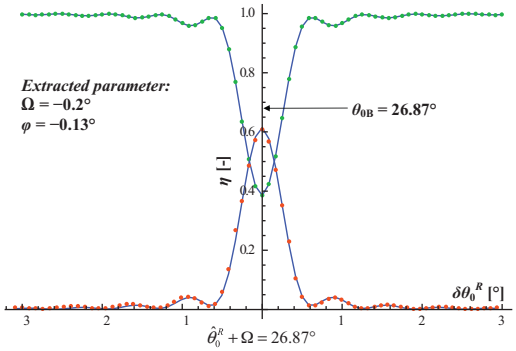

Fig. 4. Experimental data angular scan and corresponding fit of the unslanted recorded grating.

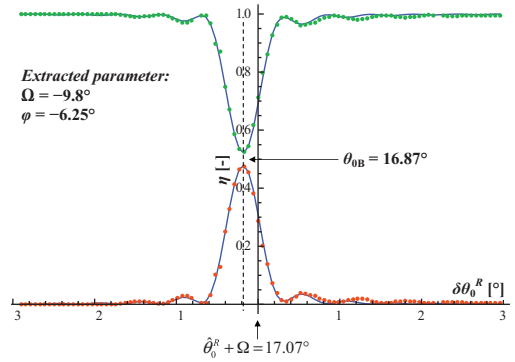

Fig. 5. Experimental data and corresponding fit to angular scan of the recorded grating with −10° pre-exposure rotated angle.